Elastic properties of CD_4 single crystals in phases I, II, and III

E. Gregoryanz* and M. J. Clouter
Department of Physics and Physical Oceanography, Memorial University of Newfoundland, St. John's, Newfoundland, Canada A1B 3X7
(Received 21 July 1998)

A technique has been developed for producing and maintaining single crystals of molecular solids of several mm^3 volume over a wide temperature range and across phase boundaries. The technique has been used in conjunction with Brillouin and Raman spectroscopy to determine the adiabatic elastic constants of single-crystal CD_4 in phases I, II, and III from 89 to 18 K along the solid-vapor saturation line. The possible space groups of CD_4-III were determined from the Brillouin data.
[S0163-1829(98)07241-5]

The unusual properties of plastic crystals have attracted considerable attention.[1,2] Usually, however, experimental measurements on such solids are very difficult, particularly over an extended temperature range. This is mainly because of a high coefficient of thermal expansion in combination with strong adhesion to the container walls which can easily give rise to mechanical strain and fracturing. Solid methane, being an archetypal plastic crystal because of its resemblance to the rare gas solids and its relative simplicity, is such a case.

At low temperatures and in equilibrium with its vapor, CD_4 exists in three phases: phase I ($Fm3m$) extends from the melting point of 89.8 K to 27.1 K; phase II ($Fm3c$) is between 27.1 and 22.1 K, and below 22.1 K lies phase III, which has a tetragonal structure[3–5] of unknown symmetry. Although CD_4 has been studied more extensively than the other isotopic variants of methane, very little is known about its elastic properties at low temperatures. The elastic constants of CD_4 were measured in phase I at 89.2 K by Brillouin spectroscopy[6] and at 85.6 K by the technique of Schaefer-Bergmann scattering.[7] In phase II the elasticity was measured by neutron scattering at $T=34.5$ and 32.5 K.[8,9] In this paper, we present measurements of the elasticity of CD_4 in phase III as well as over a wide temperature range covering all three solid phases.

Because phases II and III of CD_4 are accessible only from another solid phase, any optical experiment on a single crystal becomes a formidable task. The changes which occur in the range from 89 to 10 K are accompanied by a total volume change of $\sim 11\%$.[5] Under most circumstances this will lead to a serious level of mechanical strain and to a deterioration of sample quality which would render optical techniques unusable.

In the present case the crystals were grown from the liquid at the triple point in the presence of temperature gradient of ~ 1 K/cm between the bottom and the top of a cylindrical quartz cell of height ~ 1 cm and inner diameter 3 mm. Before any cooling was attempted the x-ray Laüe diffraction technique was used to determine the crystal orientation and ensure that the crystal was single and free of mechanical strain. A special feature of the cell was a thin, optically transparent, electrically conducting film which was deposited on the outer surface of the cell wall. The film was characterized by an intensity transmission coefficient of 70% and an electrical resistance of 10 Ω. The heat generated by passing a current through this film permitted a controlled melting of the crystal away from the cell walls. The cooling process involved simultaneous adjustment of (1) the heat dissipation in the film, (2) the rate of cooling of the crystal, and (3) the rate at which vapor was removed from the cell by pumping. When executed appropriately the result was a single crystal which was free-standing on the bottom of the cell and which could be cooled within a given solid phase without serious deterioration in optical quality. Special care was required when cooling the sample across a phase boundary, and the II-III transition was particularly difficult. Over the course of the experiments more than 30 crystals were grown and cooled to the different temperatures, but only one was successfully cooled below the second phase transition.

The light scattering measurements were carried out using a triple-pass Brillouin spectrometer[10,11] and the $\lambda_0=514.5$ nm line of an Ar^+ laser at a power level of ~ 20 mW was used as the excitation source. A 90° scattering geometry was employed and the crystal was rotated about its vertical axis in 5° or 10° intervals through a total of 70°, so that 7–12 spectra were collected at every temperature. Representative Brillouin spectra for phases I and III are shown in Fig. 1. The density of CD_4 in all three phases is known,[5] and the refractive index, which was required for the analysis process, was calculated using the Lorentz-Lorenz relation throughout the investigated temperature range.

The iterative analysis process started with a predictive calculation of the Brillouin shifts using an initial guess for the elastic constants and the results were then compared with the measured shifts. A least-squares fitting routine was then applied to minimize the difference between the measured and calculated frequency shifts by parameter searches through elastic constants space. After the best-fit set of elastic constants at every temperature was obtained it was used to generate theoretical curves of frequency shifts versus the crystal rotation angle, ϕ. These curves were then compared with the measured variation of shift versus ϕ.

For a given crystal the Brillouin shift variation with ϕ was the same at different temperatures in phases I and II. The phase transition between phases I and II was easily detected by comparatively large changes in the Brillouin shifts for the longitudinal and transverse modes. In addition, there were easily detectable changes in the Raman spectra of the two

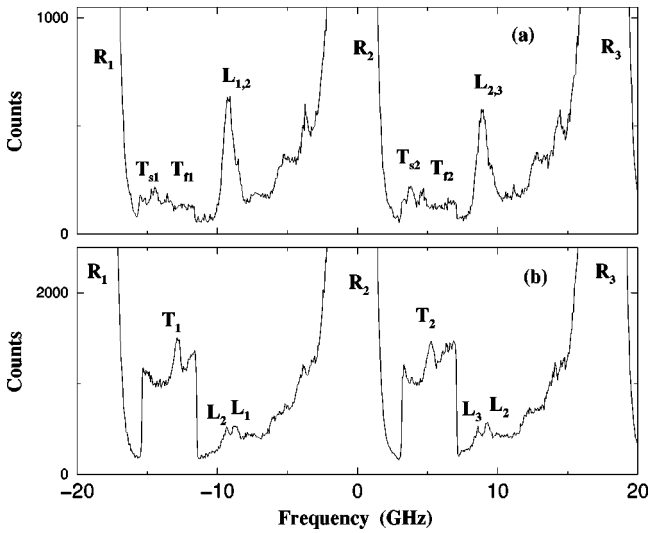

FIG. 1. Representative Brillouin spectra of CD_4 in phases I (a) and III (b). The Rayleigh peaks are labeled R_i, longitudinal L_i, where i is the number of the corresponding Rayleigh and longitudinal peak. Transverse modes are labeled $T_{(s,f)i}$ where s,f stand for slow and fast transverse modes and i shows the Rayleigh peak to which a given transverse peak belongs; the collection time for these modes was multiplied by factor 3 (a) and 10 (b).

fundamental modes ν_1 and ν_3 (see Fig. 2) which were simultaneously recorded for confirmation purposes. Because of the rotational motion present in the solid phase, the appearance of the Raman spectra is hardly changed when methane goes through the liquid-solid phase transition and even when the crystal is considerably cooled [Fig. 2(a)].

The variation of Brillouin shifts with ϕ changed slightly when the second phase transition took place. An interesting fact is that this occurred at $\sim$0.9 K above the phase transition temperature of 22.1 K which was determined by rather dramatic changes in the Raman spectra. Consequently, the

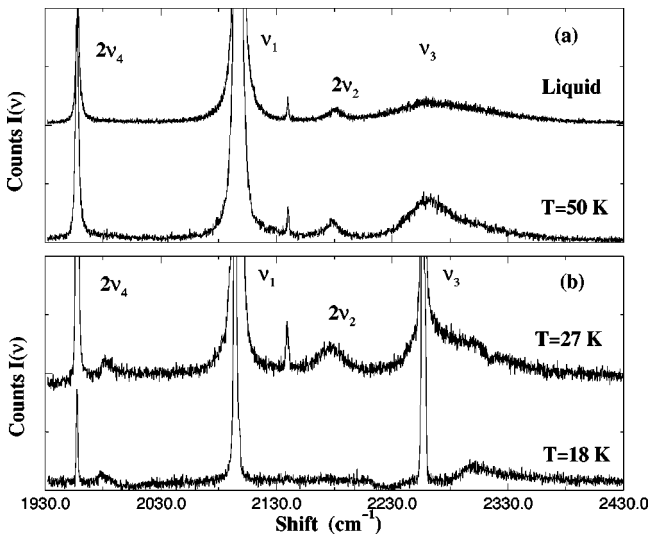

FIG. 2. Unprocessed representative Raman spectra of CD_4. All spectra but the one at T=18 K are collected without polarizer. The spectrum at $T=18$ K was collected with the polarizer axis perpendicular to the polarization vector of the scattered light. The small peak between ν_1 and $2\nu_2$ is the ν_1 line of CD_3H.

elastic constants were first calculated at 23.0 K with the assumption that the structure was still cubic. However, the fits were not good and the values of the elastic constants were very different from the values at 25 K. The final values of the elastic constants were then calculated for 23 K, and all temperatures below, using fits corresponding to the tetragonal structure.

A medium of tetragonal symmetry is known to have either seven elastic constants for the lower symmetry classes 4, $\overline{4}$, and $4/m$, or six elastic constants for the higher symmetry classes $4mm$, 422, $\overline{4}2m$, and $4/mmm$. To the best of the authors' knowledge, no information exists on the class or space group of phase III of CD_4. In an effort to resolve the issue the elastic constants were calculated assuming both of the above possibilities. The initial guesses for C_{11}, C_{12}, and C_{44} were taken to be equal to their values at the higher temperatures, and the initial values of C_{33}, C_{13}, and C_{66} were taken to be equal to the values of C_{11}, C_{12}, and C_{44} correspondingly. At all temperatures the fits for higher symmetry classes were better, and produced more consistent values for the resulting elastic constants. In both cases the agreement between calculated and measured shift was reasonably good for the range of angles where the measurements were taken. However, when the theoretical shifts for the lower symmetry case were calculated beyond the experimentally accessible range of angles, the angular distribution of Brillouin shifts for the slow transverse mode exhibited a discontinuous behavior at near-zero minima for some values of ϕ. Also, for the lower symmetry case, the values of C_{11} and C_{12} were too high compared with the values for the cubic phase at the higher temperature of 25 K, and C_{66} is negative, which contradicts the stability condition.[12] It was consequently concluded that the higher symmetry classes are the appropriate choice.

The values of the elastic constants over the investigated temperature range are listed in Table I and shown in Fig. 3. The solid circles are measured values of elastic constants which were fitted to the linear expressions shown as solid lines. C_{44} and C_{11} have steeper slopes than C_{12}, and C_{44} becomes comparable with C_{12} at the temperatures close to the first phase transition and in phases II and III. Although both phase transitions are clearly seen in the behavior of C_{11} and C_{44}, the changes of these elastic constants are fairly small. The functional dependencies of the elastic constants with temperature in phase I are very close to those of CH_4.[11] The bulk modulus in the cubic phase was calculated using $B=\frac{1}{3}(C_{11}+2C_{12})$. The bulk modulus in tetragonal phase and the aggregate shear modulus (G) in all phases were obtained from the individual elastic constants using the Voight-Reuss-Hill averaging method[13,14] [shown in Figs. 4(a) and 4(b)]. The bulk modulus increases by a factor 1.5 and the shear modulus increases by a factor of 3 across the investigated temperature range.

The elastic anisotropy A is shown in Fig. 2(c). The value $A=3.63$ at the triple point of CD_4 is high compared with rare gas solids.[6] The higher values of anisotropy (as well as the slow transverse acoustic velocity in the $\langle 110\rangle$ direction) in orientationally disordered crystals such as methane are explained by the rotation-translation coupling.[6,15] As in the case of CH_4,[11] the anisotropy slowly decreases as the tem-

TABLE I. Elastic constants of CD_4 in phase I, II, and III in kbars. Temperatures are accurate to within ± 0.2 K.

T	C_{11}	C_{12}	C_{44}	C_{33}	C_{13}	C_{66}
			Phase I			
88.2	20.6±0.2	15.3±0.1	9.5±0.1	—	—	—
70.0	23.9±0.2	17.0±0.2	11.8±0.1	—	—	—
60.0	26.7±0.2	18.7±0.2	13.4±0.1	—	—	—
50.0	27.4±0.3	18.4±0.2	14.8±0.2	—	—	—
40.0	29.0±0.3	18.5±0.2	16.5±0.2	—	—	—
35.0	30.0±0.3	18.7±0.2	16.3±0.2	—	—	—
32.0	30.0±0.3	19.0±0.2	17.4±0.2	—	—	—
29.0	31.1±0.3	18.8±0.2	18.0±0.2	—	—	—
			Phase II			
27.0	34.2±0.3	17.3±0.2	19.7±0.2	—	—	—
25.0	36.8±0.3	18.8±0.2	19.5±0.2	—	—	—
23.0[a]	38.8±0.4	19.9±0.3	17.6±0.3	39.6±0.4	12.3±0.4	9.5±0.4
			Phase III			
22.0	44.0±0.5	18.0±0.4	16.6±0.4	42.0±0.5	10.0±0.4	10.1±0.4
21.0	44.3±0.5	19.3±0.4	18.1±0.4	41.2±0.5	13.7±0.4	12.5±0.4
18.0	44.4±0.5	19.6±0.4	18.4±0.4	42.0±0.6	14.1±0.4	12.6±0.4

[a]The best fit elastic constants were first obtained for the cubic structure but the fit was not satisfactory and the values of elastic constants were not consistent with the values at the higher temperatures.

perature is lowered. In the vicinity of the phase I-II transition the anisotropy is similar to the anisotropy of rare gas solids ($A \sim 2.5$) and when the crystal enters phase III it drops to the values of ~ 1.5. The crystal appears to become more isotropic because of the decreasing rotational motion. The opposite effect of the increasing anisotropy and increasing the V_l/V_{t1} ratio with increasing high pressure was observed[16] in solid CH_4. The acoustic velocities in the high symmetry directions as a function of temperature are shown in Fig. 5. The values of velocities are slowly increasing with decreasing temperature and the values of transverse velocities in the $\langle 110 \rangle$ direction become closer to each other. The ratio of V_l/V_{t1} in $\langle 110 \rangle$ changes from ~ 3.22 to ~ 1.90, becoming comparable with the similar ratio for the rare gas solids.

By averaging over the reciprocal velocity surfaces the average longitudinal and transverse velocities were calculated. Poisson's ratio (σ) and the Debye temperature then were obtained. These parameters are shown in Figs. 6(a) and 6(b).

Integration over the Debye temperature leads to a determination of the lattice specific heat and, by combining the lattice specific heat with the known specific heat at constant pressure[17] and coefficient of volume expansion,[5] the rotational specific heat can be separated and calculated. This

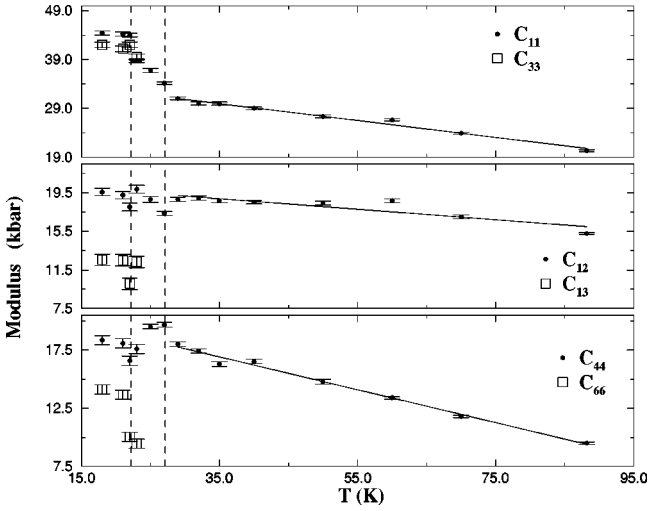

FIG. 3. Elastic constants of CD_4 as a function of temperature. The solid curves are least-squares linear fits to the data. The error bars shown represent the standard deviation in the best fit parameters and uncertainties in the frequency shift and crystal orientation. The dashed lines are positioned at phase transition temperatures of $T_{c1} = 27.1$ K and $T_{c2} = 22.1$ K.

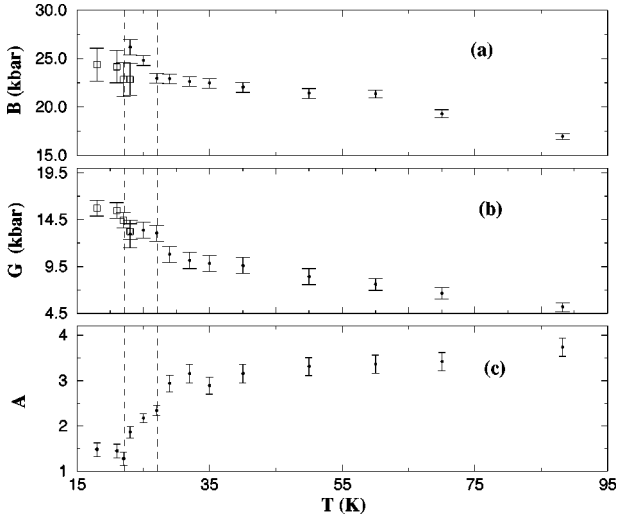

FIG. 4. Bulk (a) and shear (b) moduli and anisotropy factor (c) of CD_4 as a function of temperature. For the elastic moduli (●) are points calculated in the cubic phase, (□) calculated in tetragonal phase. The error bars shown are from the errors in elastic constants as in Fig. 3. The dashed lines are positioned as in Fig. 3.

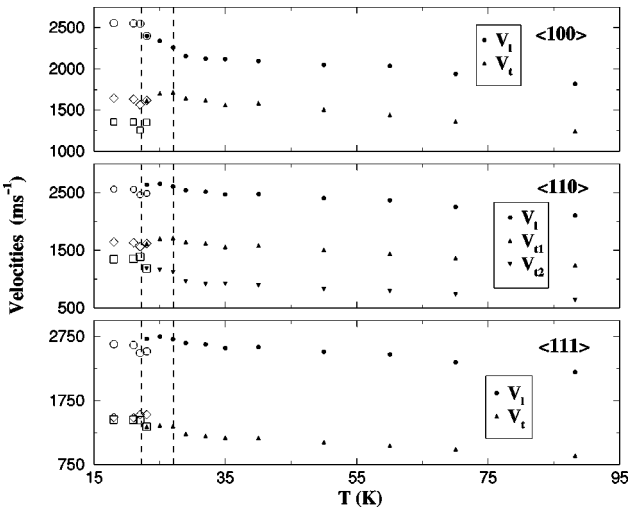

FIG. 5. Acoustic velocities of CD_4 in high symmetry directions as a function of temperature. The filled symbols are points calculated in the cubic phase and the empty symbols are points calculated in tetragonal phase. The dashed lines are positioned as in Fig. 3.

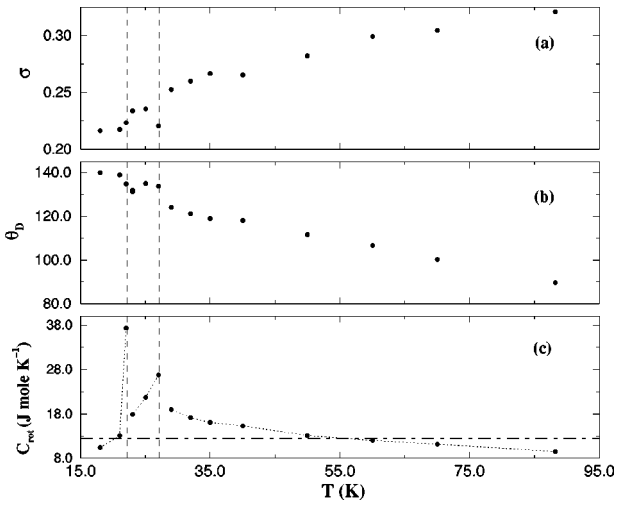

FIG. 6. (a) Poisson ratio, (b) Debye temperature, and (c) C_{rot} of CD_4. The dotted lines are guides for the eye only. The horizontal dot-dashed line is positioned at $\frac{3}{2}R$. The dashed lines are positioned as in Fig. 3.

procedure was carried out with the assumption that the rotational motion is not affected by translation. The temperature dependency of rotational specific heat is shown in Fig. 6(c). An interesting result is that in the wide temperature range from the onset of the first phase transition to $\sim$55 K the rotational specific heat is larger than $\frac{3}{2}R$. At temperatures higher than 55 K the rotational heat becomes lower than this free rotational value.

In conclusion, we obtained a complete set of data for the elastic properties of CD_4 for all three low-pressure phases. Two points that remained to be elaborated are (1) the II-III phase transition is manifested in the Brillouin spectrum at a temperature 0.9 K higher than in the Raman spectrum, and (2) the decrease in the anisotropy factor with decreasing temperature (and increasing density) is distinctly different from that observed by Shimizu, Nakashima, and Sasaki[16] for CH_4 at high pressures. It is hoped that this work will stimulate further theoretical work which may help to resolve these points.

This work was supported by a grant from the Natural Sciences and Engineering Research Council of Canada.

*Present address: Geophysical Laboratory and Center for High-Pressure Research, Carnegie Institution of Washington, 5251 Broad Branch Rd. N.W., Washington, D.C. 20005-1305.

[1] R. M. Lynden-Bell and K. H. Michel, Rev. Mod. Phys. **66**, 721 (1994).
[2] J. N. Sherwood, *The Plastically Crystalline State* (Wiley, New York, 1979).
[3] D. Bol'shutkin *et al.*, J. Struct. Chem. **12**, 313 (1971).
[4] D. R. Baer, B. A. Fraass, D. H. Riehl, and R. O. Simmons, J. Chem. Phys. **68**, 1411 (1978).
[5] A. Prokhvatilov and A. Isakina, Phys. Status Solidi A **78**, 147 (1983).
[6] S. C. Rand and B. P. Stoicheff, Can. J. Phys. **60**, 287 (1982).
[7] S. V. Marx and R. O. Simmons, J. Chem. Phys. **81**, 944 (1984).
[8] W. Press, B. Dorner, and H. Stiller, Solid State Commun. **9**, 1113 (1971).
[9] W. G. Stirling, W. Press, and H. Stiller, J. Phys. C **10**, 3959 (1977).
[10] E. Gregoryanz, M. J. Clouter, N. Rich, and R. Goulding, Phys. Rev. B **58**, 2497 (1998).
[11] E. Grigoriantz and M. J. Clouter, J. Low Temp. Phys. **111**, 717 (1998).
[12] M. Born and K. Huang, *Dynamical Theory of Crystal Lattices* (Clarendon Press, Oxford, 1954).
[13] Z. Hashin and S. Shtrikman, J. Mech. Phys. Solids **10**, 343 (1962).
[14] J. Watt and L. Peselnick, J. Appl. Phys. **111**, 1525 (1980).
[15] S. Wonneberger and A. Hüller, Z. Phys. B **66**, 191 (1987).
[16] H. Shimizu, N. Nakashima, and S. Sasaki, Phys. Rev. B **53**, 111 (1996).
[17] J. H. Colwell, E. K. Gill, and J. A. Morrison, J. Chem. Phys. **39**, 635 (1963).